SPECTRUM AWARENESS TECHNIQUES FOR 5G SATELLITE COMMUNICATIONS

A. Guidotti, D. Tarchi, V. Icolari, A. Vanelli-Coralli, G. E. Corazza

Dept. of Electrical, Electronic and Information Engineering, Univ. of Bologna, 40136 Bologna, Italy

ABSTRACT

5G communications will enable new paradigms architectures and services, and the integration of satellite and terrestrial networks can play a key role. Cognitive radios are seen as the most promising solution to dynamically cooperate, in order to exploit advanced frequency sharing techniques. To this end, efficient sensing techniques for spectrum awareness are a must. In this paper, we provide preliminary results on energy detection (ED) and cyclostationary feature detection (CFD) algorithms applied to a downlink Ka-band scenario. These results show that coexistence between satellite and terrestrial networks is possible and cognitive radios can ease their integration in future 5G communications.

Index Terms— 5G, Satellite Communications, Cognitive Radio, Spectrum Sensing

1. INTRODUCTION

Future 5G Wireless Communication systems aim at realizing an ubiquitous ultra-broadband network that will provide highly efficient, ultra-reliable, dependable, secure, privacy preserving and delay critical services to everyone [1]. There are many challenges that 5G networks shall address, in terms of key performance indicators, *e.g.*, a large throughput increase (1000x in aggregate and 10x at link level), low service-level latency (*e.g.*, 1 ms for tactile Internet), an extremely high energy efficiency, global and seamless connectivity, completely redesign architectures and services, etc. Furthermore, 5G infrastructures will also need to be extremely flexible, so as to meet both foreseen and unknown requirements and to align with stakeholders' expectations. In order to cope with these requirements, 5G systems foresee a deeper integration of terrestrial and satellite networks than what has been already done during the last years.

The integration of SatCom and terrestrial networks can play a key role in 5G systems from several point of view. Due to their inherent large footprint, satellites can complement and extend dense terrestrial networks, by providing larger cells in a heterogeneous arrangement that can be used for emergency scenarios as well. SatCom can also efficiently provide backhaul services to terrestrial networks in particular in remote areas, as well as improve the Quality of Experience (QoE) by means of intelligent routing that can off-load traffic from terrestrial networks. Future satellite systems (2020–2025) are expected to exploit larger GEO satellites, with capacities ranging from hundreds of Gbps up to Tbps. This will be achieved by means of hundreds of spotbeams, via higher order frequency reuse. In fact, the limited amount of exclusive spectrum that can be accessed by the Fixed Satellite Service (FSS) limits the actual system capacity. Current High Throughput Satellites (HTS) in Ka-band and above have gained momentum to reduce the large cost per bit and allow Ka-band satellites to provide the required capacity [2–4]. Higher frequency bands will also be used: for broadband satellites, it has been proposed to move feeder links up to Q/V bands, and focus is also on finding additional spectrum for the user link in Ka-band.

In this context, frequency sharing between terrestrial and satellite networks would provide great benefits to both. Cognitive Radio (CR) techniques are seen as the most promising mean to tackle the spectrum scarcity problem [5]. They allow to efficiently share some portions of the spectrum while limiting harmful interference among different communication systems. CRs potential has already been demonstrated in wireless terrestrial services [6], while in SatCom their implementation and study is still in its infancy. SatComs represent a challenging application scenario for CRs, due to, *e.g.*, the geographically wide coverage of the spectrum allocation and the power imbalance among ground and user terminals.

In this paper, we focus on spectrum sensing techniques for a SatCom downlink Ka-band scenario [7]. Among several Spectrum Sensing techniques [5], we will focus on energy detection and cyclostationary feature detection, that are described and assessed in the considered scenario. Simulation results show that CR-based satellite systems can significantly improve spectrum utilization, which would enable the integration between terrestrial and satellite networks in 5G, as well as provide additional spectrum for both systems.

2. REFERENCE SCENARIO

ITU-R allocates the 19.7–20.2 GHz and 29.5–30 GHz bands to downlink (DL) and uplink (UL) satellite systems, respectively, on an exclusive basis, also allowing uncoordinated FSS

This work was partially supported supported by the EU FP7 project CoRaSat (FP7 ICT STREP Grant Agreement n. 316779).

978-0-9928626-3-3/15/$31.00 ©2015 IEEE

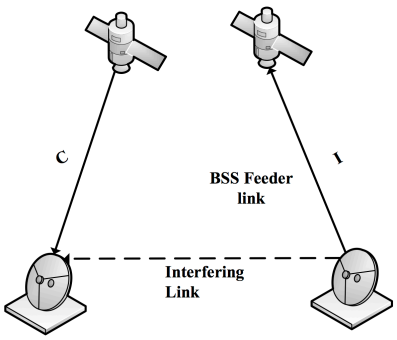

Fig. 1: Reference SatCom DL scenario in the 17.3–17.7 GHz band (C: cognitive link, I: incumbent link).

terminals. Other parts of the Ka-band are also allocated to FSS on a non-exclusive basis, as they are shared with Fixed Service (FS) and Broadcasting Satellite System (BSS) feeder links [8]. Within CEPT, ITU-R allocations are followed and extended. In particular, Decision ECC/DEC/(05)08 [9] establishes that the band from 17.3 to 17.7 GHz is allocated without prejudice to the use by BSS feeder UL and no terrestrial service is allocated on an incumbent basis. CR techniques are considered the most promising mean to allow different systems to share spectrum without interfering with each other, exploting the spectrum made available by Radio Regulations. In this paper, we consider the SatCom DL scenario in the 17.3–17.7 GHz Ka-band depicted in Fig.1 [7, 10]. The BSS feeder links are the incumbent service, while cognitive uncoordinated FSS links are also allowed. Interference generated from the cognitive FSS satellite towards the incumbent receiver (BSS satellite) is negligible: since the FSS and BSS satellites occupy two separate orbital positions, interference is inherently avoided thanks to the actual antenna pointing. In this scenario, coexistence between FSS DL and BSS feeder links is thus limited by the interference generated from the incumbent system towards the FSS terminal. In particular, a significant amount of aggregate interference may occur at a given FSS terminal due to the side-lobes of the receiving antenna pattern. CR techniques can thus be employed to foster the coexistence between FSS DL and BSS feeder links, as shown in the following sections. In the following, it is assumed that the receiving chain at the cognitive terminal is used for both sensing and secondary transmissions.

3. SPECTRUM AWARENESS TECHNIQUES

Spectrum sensing (SS) aims at detecting the incumbent user signal by scanning a selected frequency band B [5,6]. It refers to the detection of an unknown or partially known signal, and a trade-off between the probability of false alarm (P_f) and the probability of detection (P_d) is necessary for achieving an accurate degree of certainty in such detection. SS techniques can be modeled as a binary hypothesis test problem, comparing a statistical metric with a given threshold.

3.1. Energy detection

An energy detector (ED) aims at detecting the presence of incumbent signals based on the energy estimated at the antenna input of the cognitive terminal [11, 12]. It is a blind detection technique, as it does not require *a-priori* knowledge on the incumbent signal, and therefore has a general applicability in CR-based systems. However, it is highly susceptible to Signal-to-Noise Ratio (SNR) wall problem, that prevents from achieving the desired target probabilities P_d or P_f, as the uncertainty in noise power estimation, ρ_N, can easily erroneously trigger the detection [13, 14].

We consider two different ED techniques: i) Constant False Alarm Probability (CFAR), in which P_f is fixed and parameters are set so as to reach the desired probability of detection; and ii) Constant Detection Rate (CDR), where P_d is fixed and a target probability of false alarm shall be reached. From [15], P_d and P_f are given by (1) at the top of next page, where $\mathcal{Q}(\cdot)$ is the Marcum Q-function, γ_{thr} is the detection threshold, σ^2 is the noise variance, $N_{oss} = 2BT_{oss}$ is the number of observed samples, and γ is the SNR at the end of the receiving RF chain (*i.e.*, it includes the RF chain noise). A critical parameter is the sensing (observation) time, T_{oss}, related to N_{oss}. It shall be set in both the minimum and the maximum value, which are related to the desired P_d or P_f and the fragmentation between sensing time and cognitive transmission, respectively. The latter relation is motivated by the assumption that the same receiving chain is used for both sensing and transmission. Moreover, the cognitive terminal characteristics, *e.g.*, sensed bandwidth, distance from incumbent user(s), receiver chain, etc., influence the energy detector performance as well. By inverting (1), the normalized detection thresholds for CFAR and CDR are given by the second terms in (1), where $\hat{\gamma}$ is the SNR value that allows to meet the target probabilities $\hat{P}_d$ and $\hat{P}_f$, *i.e.*, for all SNR values above $\hat{\gamma}$, the target probability of detection is guaranteed. The parameters used for numerical simulations are listed in Table 1, while further details for the satellite system set up are available in [7]. The detection thresholds have been computed by also taking into account additional noise contributions as specified in ITU-R Radio Regulations [8], in particular receiving system noise, fade margin, and the UL contribution to the overall satellite link noise (short-term interference). ITU-R also specifies values of I/N (Interference-to-Noise Ratio) related to the maximum allowable error performance and availability degradation of digital satellite paths arising from interference for systems below 30 GHz [16], and in this paper we consider a maximum value of -10 dB that shall not be exceeded for more than 9.5% of the year. All of these factors are included in γ in (1).

Fig. 3 shows, in the CFAR case, P_d as a function of the SNR γ for the values of observation time and P_s shown in Table 1.

$$P_f = \mathcal{Q}\left(\frac{\gamma_{thr}-\sigma^2}{\sqrt{\frac{2}{N_{oss}}}\sigma^2}\right) \longrightarrow \gamma_{thr}^{(CFAR)} = \sqrt{\frac{2}{N_{oss}}}\mathcal{Q}^{-1}\left(\hat{P}_f\right)+1$$
$$P_d = \mathcal{Q}\left(\frac{\frac{\gamma_{thr}}{\sigma^2}-(\gamma+1)}{\sqrt{\frac{2}{N_{oss}}}(\gamma+1)}\right) \longrightarrow \gamma_{thr}^{(CDR)} = (\hat{\gamma}+1)\left(\sqrt{\frac{2}{N_{oss}}}\mathcal{Q}^{-1}\left(\hat{P}_d\right)+1\right) \quad (1)$$

$$\mathcal{S}_x^{\alpha}(f) = \sum_{\tau=-\infty}^{+\infty} \mathcal{R}_x^{\alpha}(\tau)e^{-j2\pi f\tau} \quad (2)$$
$$\mathcal{I}(\alpha) = \max_f |\mathcal{S}_x^{\alpha}(f)|$$

Table 1: Simulation parameters.

Parameter	Value	Units
Target P_d	0.9	
Target P_f	0.1	
Sensing time T_{oss}	0.6	ms
$\gamma_{thr}^{(CFAR)}$	1.0331	
$\gamma_{thr}^{(CDR)}$	1.0636	
Sensed bandwidth	5	MHz
FSS terminal (LAT,LON)	(51.73N,0.17W)	deg.
FSS satellite LON	53E	deg.

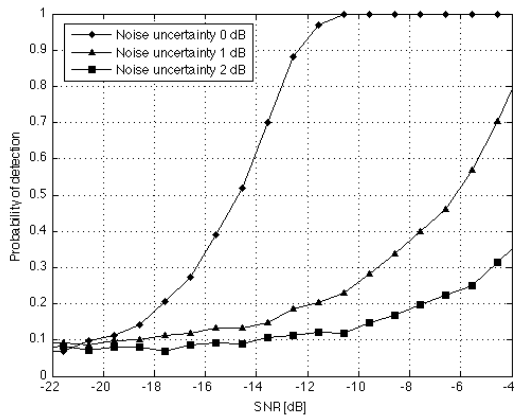

Fig. 3: CFAR: P_d with $P_f = 0.1$ as a function of γ and ρ_N.

In this case, noise uncertainty worsens the probability of detection and, thus, the target performance can be achieved by increasing the T_{oss}. However, the SNR wall phenomenon prevents from achieving the target P_d in high noise uncertainty scenarios, even with long sensing periods. Fig. 4 shows the minimum observation time T_{oss} as a function of γ, such that the target performance is guaranteed. The asymptotic effect of the SNR wall on the sensing time is clearly visible.

In the CDR approach, $\gamma_{thr}^{(CDR)}$ is set to guarantee the desired P_d for the I/N threshold. Since P_f depends on the sensing time only, it is more interesting to show the guaranteed probability as a function of T_{oss}, as in Fig. 5. Moreover, since the CDR methodology guarantees a target P_d for all of the SNR values above a certain threshold, it is possible to avoid evaluation for different values of γ. In this case as well, the SNR wall phenomenon is present for strong noise uncertainties introducing an asymptote at about 0.5 for P_f. It is thus possible to state that, by fixing $\gamma_{thr}^{(CFAR)}$ and $\gamma_{thr}^{(CDR)}$, noise uncertainties do not allow to guarantee the desired probabilities. If we consider an ideal case with no or very small errors in noise estimation, the choice between CFAR and CDR is given by the trade-off in spectrum efficiency: if the focus is on maximizing spectrum exploitation, even if an incumbent user is present but not detected, the CFAR methodology would be preferred rather than the CDR, which mainly aims at avoiding interference towards the incumbent users, at the expense of spectrum exploitation.

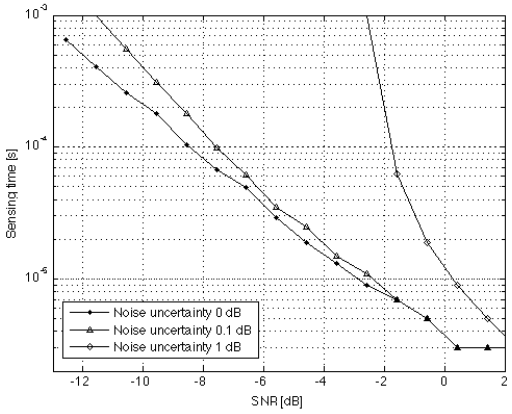

Fig. 4: CFAR: T_{oss} to achieve the target P_d as a function of γ and ρ_N.

Once the proper detection threshold has been set, taking into account the trade-off between spectrum utilization and interference avoidance, as well as the effect of the SNR wall, it is possible to define a map showing the available bands. In particular, the whole 17.3–17.7 GHz band is analyzed in 11 sub-bands, each 36 MHz wide. This is performed by also taking into account the location of the FSS terminal, the longitude of the satellite at which the terminal points, and the sensing bandwidth (see Table 1). Figg. 6-7 compare the frequency availability of the CFAR and CDR approaches, assuming $\rho_N = 0$ dB. It can be noticed that CFAR guarantees that the vacant bands (white) will be not identified as occupied (black), *i.e.*, the ED chooses for the presence of the incumbent

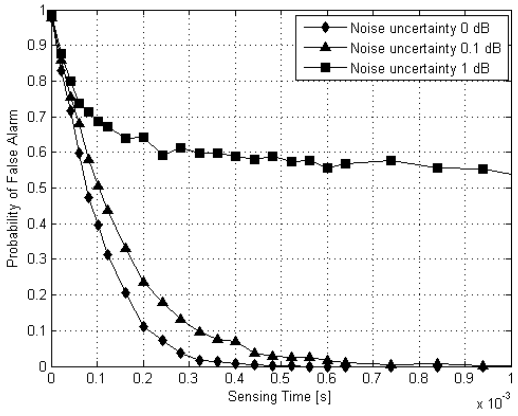

Fig. 5: CDR: P_f as a function of T_{oss} and ρ_N, $I/N = -10$ dB.

user when the band in vacant with a percentage lower than the target P_f. However, in order to guarantee with a certain probability that occupied bands will not be identified as vacant, it is necessary to sense for a longer time as shown in the fifth band, in which a transition between false alarm and detection can be highlighted. On the contrary, a CDR approach guarantees that the occupied bands are detected with a probability higher than the target P_d but, in order to identify the vacant bands, it will be necessary to sense for a longer period.

3.2. Cyclostationary feature detection

Differently from the energy detector, a cyclostationary feature detector (CFD) exploits periodic features that are implicitly present in the signal, due to, *e.g.*, pilots, preambles, cyclic prefixes, modulation schemes, etc [17]. A CFD allows to discern among different incumbent signals, thus not only detecting whether they are present or not, but also distinguishing them from noise, which has no cyclic features. Thus, the SNR wall phenomenon is not present, and the CFD provides good performance in low SNR regimes. On the other hand, it is quite complex from a computational point of view, as it requires the computation of the Fourier series of the autocorrelation function of the incoming signal: this function presents peaks in the frequency domain at multiples of some *cyclic frequencies*, which are related to the built-in periodicity of the signal. By building the *Spectral Correlation Density* (SCD) function, these second-order correlations can be detected, thus allowing to discern among different type of signals and between incumbent signals and noise. The SCD $\mathcal{S}_x^{\alpha}(f)$ is given by (2), where $\{\mathcal{R}_x^{\alpha}(\tau)\}_{\tau=-\infty}^{+\infty}$ are the Fourier series coefficients of the signal autocorrelation function, α is the generic cyclic frequency, and $x(t)$ is the incoming signal. In the considered scenario, the incumbent signal is a DVB-S2 like signal, and thus the following periodicities can be detected: i) Start of Frame sequence, which is always present; ii) pilot sequences,

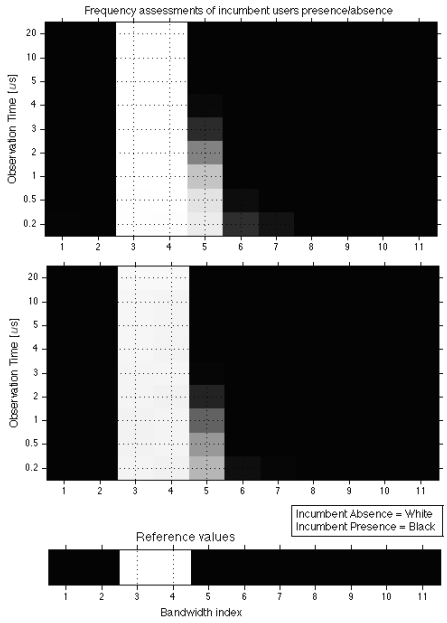

Fig. 6: CFAR: frequency assessment ($\rho_N = 0$ dB, $P_f = 0.01$ above, $P_f = 0.1$ below).

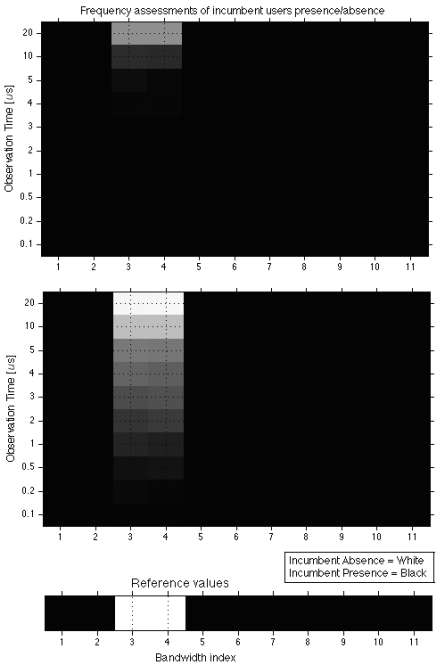

Fig. 7: CDR: frequency assessment ($\rho_N = 0$ dB, $P_d = 0.99$ above, $P_d = 0.9$ below).

Table 2: Simulation parameters for cyclostationary detection assessment.

Parameter	Value	Units
Incumbent modulation	4-QAM	
Symbol rate	$5 \cdot 10^6$	Baud
Sampling frequency f_s	$50 \cdot 10^6$	Hz
Frequency res.	$f_s/512$	Hz
Cyclic frequency res.	$f_s/1024$	Hz
Observation time	$10^{-6}, 10^{-5}, 10^{-4}$	s

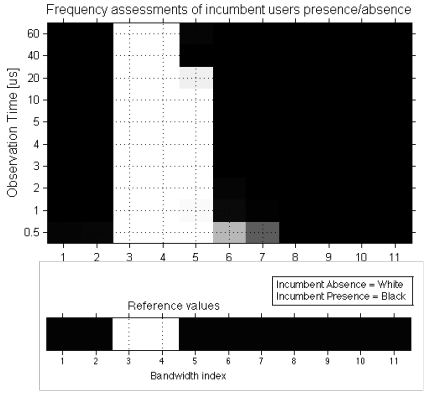

Fig. 8: CFD: frequency assessment ($\rho_N = 0$ dB, $P_f = 0.1$).

which are optional; and iii) different modcod schemes. These periodicited can be detected by means of the *cyclic profile domain* $\mathcal{I}(\alpha)$, defined in (2). The parameters used for the performance assessment of the CFD are provided in Table 2. The signal, if present, will show peaks at all the multiple integers of the symbol rate.

Fig. 8 shows the frequency availability obtained with the CFD with $\rho_N = 0$ dB and targeting $P_f = 0.1$. Compared to Fig. 6, it can be noticed that the same sub-bands are identified as available. However, this detector requires longer observation periods to converge to the correct detection (20μs compared to 4μs in the ED case). This confirms that the CFD needs larger values of T_{oss}, but it allows to distinguish the different type of incumbent signals. Moreover, the CFD does not suffer from the SNR wall phenomenon, and thus provides good performance in slow SNR regimes as well.

4. CONCLUSIONS

In this paper, we analyzed the performance of energy detection and cyclostationary feature detection in a downlink SatCom Ka-band scenario, providing an insight on the advantages and disadvantages of both. Performance results show that the considered spectrum sensing techniques can be implemented to foster frequency sharing between satellite and terrestrial networks. This would provide great benefits to both systems, and ease their integration in future 5G communication systems. It is worthwhile noting that, in this scenario, coexistence between FSS and BSS is limited by the interference generated from the incumbent system towards the FSS terminal. Thus, it would be beneficial to also perform an estimation of the interference received from incumbent trasmitters, in order to define the Quality-of-Service with which the available bands can be accessed by the cognitive FSS terminal. This work is currently ongoing, and some preliminary results are available in [18].

REFERENCES

[1] 5G Infrastructure Association, Vision White Paper, "The 5G Infrastructure Public Private Partnership: the next generation of communication networks and services," Feb. 2015.

[2] Eutelsats KA-SAT, [online]. Available: http://www.eutelsat.com/

[3] VIASAT ViaSat-1, [online]. Available: https://www.viasat.com

[4] SES SES-12, [online]. Available: http://www.ses.com/

[5] S. Haykin, "Cognitive radio: brain-empowered wireless communications," *IEEE JSAC*, vol. 23, no. 2, pp. 201–220, Feb. 2005.

[6] E. Hossain, D. Niyato, and Z. Han, "Dynamic Spectrum Access and Management in Cognitive Radio Networks," Cambirdge University Press, Cambridge, UK, 2009.

[7] EU FP7 Project CoRaSat (COgnitive RAdio for SATellite Communications), http://www.ict-corasat.eu/

[8] ITU-R Standard, "Radio Regulations – Volume 1: Articles," 2012.

[9] ECC Decision ECC/DEC/(05)08, "The availability of frequency bands for high density applications in the Fixed-Satellite Service (space-to- Earth and Earth-to-space)," amended Mar. 2013.

[10] S. Maleki, S. Chatzinotas, B. Evans, K. Liolis, J. Grotz, A. Vanelli-Coralli, and N. Chuberre, "Cognitive Spectrum Utilization in Ka Band Multibeam Satellite Communications," *to appear in IEEE Comm. Mag.*, 2014.

[11] H. Urkowitz, "Energy detection of unknown deterministic signals," *Proc. of the IEEE*, vol. 55, no. 4, pp. 523–531, Apr. 1967

[12] E. Axell, G. Leus, E. G. Larsson, and H. V. Poor, "Spectrum Sensing for Cognitive Radio: State-of-the-Art and Recent Advances," *IEEE* Sig. Proc. Mag., vol. 29, no. 3, pp. 101–116, Mat 2012.

[13] D. Cabric, S. M. Mishra, and R. W. Brodersen, "Implementation issues in spectrum sensing for cognitive radios," *Proc. of the 38th Asilomar Conference on Signals, Systems and Computers*, pp. 772–776, Nov. 2004.

[14] H. Kim and K. G. Shin, "In-Band Spectrum Sensing in IEEE 802.22 WRANs for Incumbent Protection," *IEEE Trans. on Mob. Comp.*, vol. 9, no. 12, pp. 1766–1779, Dec. 2012.

[15] R. Tandra and A. Sahai, "SNR Walls for Signal Detection," *IEEE J. on Sel. Topics in Sig. Proc.*, vol. 2, no. 1, pp. 4–17, Feb. 2008.

[16] ITU-R Recommendation S.1432-1, *Apportionment of the allowable error performance degradations to fixed-satellite service (FSS) hypothetical reference digital paths arising from time invariant interference for systems operating below 30 GHz*, 2006.

[17] J. Lunden, V. Koivunen, A. Huttunen, and H. V. Poor, "Spectrum Sensing in Cognitive Radios based on Multiple Cyclic Frequencies," *Proc. of CROWNCOM*, pp. 37–42, Aug. 2007.

[18] V. Icolari, A. Guidotti, D. Tarchi, and A. Vanelli-Coralli, "An Interference Estimation Technique for Satellite Cognitive Radio Systems," *to appear in ICC 2015*, Jun. 2015.